

Original citation:

Xu, Tianhua, Jacobsen, Gunnar, Popov, Sergei, Li, Jie, Friberg, Ari T. and Zhang, Yimo. (2011) Analytical estimation of phase noise influence in coherent transmission system with digital dispersion equalization. *Optics Express*, 19 (8). pp. 7756-7768.

Permanent WRAP URL:

<http://wrap.warwick.ac.uk/93889>

Copyright and reuse:

The Warwick Research Archive Portal (WRAP) makes this work by researchers of the University of Warwick available open access under the following conditions. Copyright © and all moral rights to the version of the paper presented here belong to the individual author(s) and/or other copyright owners. To the extent reasonable and practicable the material made available in WRAP has been checked for eligibility before being made available.

Copies of full items can be used for personal research or study, educational, or not-for-profit purposes without prior permission or charge. Provided that the authors, title and full bibliographic details are credited, a hyperlink and/or URL is given for the original metadata page and the content is not changed in any way.

Publisher's statement:

© 2011 Optical Society of America. One print or electronic copy may be made for personal use only. Systematic reproduction and distribution, duplication of any material in this paper for a fee or for commercial purposes, or modifications of the content of this paper are prohibited. <http://dx.doi.org/10.1364/OE.19.007756>

A note on versions:

The version presented here may differ from the published version or, version of record, if you wish to cite this item you are advised to consult the publisher's version. Please see the 'permanent WRAP URL' above for details on accessing the published version and note that access may require a subscription.

For more information, please contact the WRAP Team at: wrap@warwick.ac.uk

Analytical estimation of phase noise influence in coherent transmission system with digital dispersion equalization

Tianhua Xu,^{1,2,3,*} Gunnar Jacobsen,² Sergei Popov,¹ Jie Li,²
Ari T. Friberg,¹ and Yimo Zhang³

¹Royal Institute of Technology, Stockholm, SE-16440, Sweden

²Acreo AB, Electrum 236, SE-16440, Kista, Sweden

³Tianjin University, Tianjin, 300072, China

*tianhua@kth.se

Abstract: We present a novel investigation on the enhancement of phase noise in coherent optical transmission system due to electronic chromatic dispersion compensation. Two types of equalizers, including a time domain fiber dispersion finite impulse response (FD-FIR) filter and a frequency domain blind look-up (BLU) filter are applied to mitigate the chromatic dispersion in a 112-Gbit/s polarization division multiplexed quadrature phase shift keying (PDM-QPSK) transmission system. The bit-error-rate (BER) floor in phase estimation using an optimized one-tap normalized least-mean-square (NLMS) filter, and considering the equalization enhanced phase noise (EPPN) is evaluated analytically including the correlation effects. The numerical simulations are implemented and compared with the performance of differential QPSK demodulation system.

©2011 Optical Society of America

OCIS codes: (060.1660) Coherent communications; (060.2330) Fiber optics communications.

References and links

1. P. S. Henry, "Lightwave primer," *IEEE J. Quantum Electron.* **21**(12), 1862–1879 (1985).
2. G. P. Agrawal, *Fiber-optic communication systems 3rd Edition* (John Wiley & Sons, Inc., 2002), Chap. 2.
3. J. G. Proakis, *Digital communications 5th Edition* (McGraw-Hill Companies, Inc., 2008), Chap. 10.
4. H. Bulow, F. Buchali, and A. Klekamp, "Electronic dispersion compensation," *J. Lightwave Technol.* **26**(1), 158–167 (2008).
5. M. G. Taylor, "Coherent detection method using DSP for demodulation of signal and subsequent equalization of propagation impairments," *IEEE Photon. Technol. Lett.* **16**(2), 674–676 (2004).
6. Y. Han, and G. Li, "Coherent optical communication using polarization multiple-input-multiple-output," *Opt. Express* **13**(19), 7527–7534 (2005).
7. G. Goldfarb, and G. Li, "Chromatic dispersion compensation using digital IIR filtering with coherent detection," *IEEE Photon. Technol. Lett.* **19**(13), 969–971 (2007).
8. X. Zhou, J. Yu, D. Qian, T. Wang, G. Zhang, and P. D. Magill, "High-spectral-efficiency 114-Gb/s transmission using PolMux-RZ-8PSK modulation format and single-ended digital coherent detection technique," *J. Lightwave Technol.* **27**(3), 146–152 (2009).
9. E. Ip, A. P. T. Lau, D. J. F. Barros, and J. M. Kahn, "Coherent detection in optical fiber systems," *Opt. Express* **16**(2), 753–791 (2008).
10. E. M. Ip, and J. M. Kahn, "Fiber impairment compensation using coherent detection and digital signal processing," *J. Lightwave Technol.* **28**(4), 502–519 (2010).
11. M. G. Taylor, "Phase estimation methods for optical coherent detection using digital signal processing," *J. Lightwave Technol.* **27**(7), 901–914 (2009).
12. D. S. Ly-Gagnon, S. Tsukamoto, K. Katoh, and K. Kikuchi, "Coherent detection of optical quadrature phase-shift keying signals with carrier phase estimation," *J. Lightwave Technol.* **24**(1), 12–21 (2006).
13. Y. Mori, C. Zhang, K. Igarashi, K. Katoh, and K. Kikuchi, "Unrepeated 200-km transmission of 40-Gbit/s 16-QAM signals using digital coherent receiver," *Opt. Express* **17**(3), 1435–1441 (2009).
14. W. Shieh, and K. P. Ho, "Equalization-enhanced phase noise for coherent-detection systems using electronic digital signal processing," *Opt. Express* **16**(20), 15718–15727 (2008).
15. A. P. T. Lau, W. Shieh, and K. P. Ho, "Equalization-enhanced phase noise for 100Gb/s transmission with coherent detection," in *Proceedings of OptoElectronics and Communications Conference* (Hong Kong, 2009), paper FQ3.

16. A. P. T. Lau, T. S. R. Shen, W. Shieh, and K. P. Ho, "Equalization-enhanced phase noise for 100 Gb/s transmission and beyond with coherent detection," *Opt. Express* **18**(16), 17239–17251 (2010).
17. K. P. Ho, A. P. T. Lau, and W. Shieh, "Equalization-enhanced phase noise induced timing jitter," *Opt. Lett.* **36**(4), 585–587 (2011).
18. C. Xie, "Local oscillator phase noise induced penalties in optical coherent detection systems using electronic chromatic dispersion compensation," in *Proceeding of IEEE Conference on Optical Fiber Communication* (San Diego, California, 2009), paper OMT4.
19. C. Xie, "WDM coherent PDM-QPSK systems with and without inline optical dispersion compensation," *Opt. Express* **17**(6), 4815–4823 (2009).
20. I. Fatadin, and S. J. Savory, "Impact of phase to amplitude noise conversion in coherent optical systems with digital dispersion compensation," *Opt. Express* **18**(15), 16273–16278 (2010).
21. S. Oda, C. Ohshima, T. Tanaka, T. Tanimura, H. Nakashima, N. Koizumi, T. Hoshida, H. Zhang, Z. Tao, and J. C. Rasmussen, "Interplay between Local oscillator phase noise and electrical chromatic dispersion compensation in digital coherent transmission system," in *Proceeding of IEEE European Conference on Optical Communication* (Torino, Italy, 2010), paper Mo.1.C.2.
22. S. J. Savory, "Digital filters for coherent optical receivers," *Opt. Express* **16**(2), 804–817 (2008).
23. S. J. Savory, "Compensation of fibre impairments in digital coherent systems," in *Proceeding of IEEE European Conference on Optical Communication* (Brussels, Belgium, 2008), paper Mo.3.D.1.
24. M. Kuschnerov, F. N. Hauske, K. Piyawanno, B. Spinnler, A. Napoli, and B. Lankl, "Adaptive chromatic dispersion equalization for non-dispersion managed coherent systems," in *Proceeding of IEEE Conference on Optical Fiber Communication* (San Diego, California, 2009), paper OMT1.
25. R. Kudo, T. Kobayashi, K. Ishihara, Y. Takatori, A. Sano, and Y. Miyamoto, "Coherent optical single carrier transmission using overlap frequency domain equalization for long-haul optical systems," *J. Lightwave Technol.* **27**(16), 3721–3728 (2009).
26. www.vpiphotonics.com
27. S. Haykin, *Adaptive filter theory 4th Edition* (Prentice Hall, 2001).
28. S. Benedetto, E. Biglieri, and V. Castellani, *Digital transmission theory* (Prentice-Hall, Inc., 1987), Chap.5.
29. G. Jacobsen, "Laser phase noise induced error rate floors in differential n-level phase-shift-keying coherent receivers," *Electron. Lett.* **46**(10), 698–700 (2010).
30. E. Vanin, and G. Jacobsen, "Analytical estimation of laser phase noise induced BER floor in coherent receiver with digital signal processing," *Opt. Express* **18**(5), 4246–4259 (2010).
31. S. J. Savory, "Digital signal processing options in long haul transmission," in *Proceeding of IEEE Conference on Optical Fiber Communication* (San Diego, California, 2008), paper OTuO3.
32. C. R. S. Fludger, T. Duthel, D. van den Borne, C. Schullien, E.-D. Schmidt, T. Wuth, J. Geyer, E. De Man, Khoe Giok-Djan, and H. de Waardt, "Coherent equalization and POLMUX-RZ-DQPSK for robust 100-GE transmission," *J. Lightwave Technol.* **26**(1), 64–72 (2008).
33. T. Xu, G. Jacobsen, S. Popov, J. Li, E. Vanin, K. Wang, A. T. Friberg, and Y. Zhang, "Chromatic dispersion compensation in coherent transmission system using digital filters," *Opt. Express* **18**(15), 16243–16257 (2010).
34. G. Goldfarb, M. G. Taylor, and G. Li, "Experimental demonstration of fiber impairment compensation using the split-step finite-impulse-response filtering method," *IEEE Photon. Technol. Lett.* **20**(22), 1887–1889 (2008).
35. F. Yaman, and G. Li, "Nonlinear impairment compensation for polarization-division multiplexed WDM transmission using digital backward propagation," *IEEE Photon. J.* **1**(2), 144–152 (2009).

1. Introduction

The performance of high speed optical fiber transmission systems is severely affected by chromatic dispersion (CD), polarization mode dispersion (PMD), phase noise (PN) and nonlinear effects [1–4]. Coherent optical detection allows the significant equalization of transmission system impairments in the electrical domain, and has become one of the most promising techniques for the next generation communication networks [4–10]. With the full optical field information, the fiber dispersion and carrier phase noise can be well compensated by the efficient digital signal processing (DSP). Several feed-forward and feed-back carrier phase estimation (CPE) algorithms have been validated as effective methods for mitigating the phase fluctuation from the laser sources [9–13]. However, the analysis of the phase noise in the transmitter (TX) and the local oscillator (LO) lasers is often lumped together in these algorithms, and the influence of the large chromatic dispersion on the phase noise in the system is not considered.

Related work has been developed to deliberate the interplay between the digital chromatic dispersion equalization and the laser phase noise [14–21]. W. Shieh, K. P. Ho and A. P. T. Lau et al. have provided the theoretical assessment and analysis to evaluate the equalization enhanced phase noise (EEPN) from the interaction between the LO phase fluctuation and the

fiber dispersion in coherent transmission system [14–17]. C. Xie has investigated the impact of chromatic dispersion on both the LO phase noise to amplitude noise conversion and the fiber nonlinear effects [18,19]. I. Fatadin and S. J. Savory have also studied the influence of the equalization enhanced phase noise in QPSK, 16-level quadrature amplitude modulation (16-QAM) and 64-QAM coherent transmission systems by employing the time-domain CD equalization [20]. Due to the existence of EEPN, the requirement of laser linewidth cannot be generally relaxed for the transmission system with higher symbol rate. It would be of interest to investigate in more detail the bit-error-rate (BER) performance of the equalization enhanced phase noise in the coherent optical communication system employing electronic chromatic dispersion compensation.

In this paper, we present a detailed analysis on the impact of the dispersion equalization enhanced phase noise in the coherent transmission system using two electronic dispersion equalizers: a time domain fiber dispersion finite impulse response (FD-FIR) filter and a frequency domain blind look-up (BLU) filter [22–25]. The investigation is performed in a 112-Gbit/s non-return-to-zero polarization division multiplexed quadrature phase shift keying (NRZ-PDM-QPSK) transmission system, which is implemented in the VPI simulation platform [26]. The carrier phase estimation is realized by using a one-tap normalized least mean square (NLMS) filter [13,27], of which the leading order performance is analytically described. Using the FD-FIR and the BLU equalization, the bit-error-rate floor in the NLMS-CPE considering the EEPN is analytically evaluated. Simulation results are used to validate the error-rate floor prediction based upon the theoretical analysis. As an important reference case, a 28-Gsymbol/s differential QPSK (DQPSK) transmission system is also implemented for differential phase detection, of which the basic theory is already reported [28–30]. The CPE performance of the one-tap NLMS digital filter and the differential phase demodulation are comparatively analyzed.

2. Principle of equalization enhanced phase noise

The scheme of the coherent optical communication system with digital CD equalization and carrier phase estimation is depicted in Fig. 1. The transmitter laser signal including the phase noise passes through both transmission fibers and the digital CD equalization module, and so the net dispersion experienced by the transmitter PN is close to zero. However, the local oscillator phase noise only goes through the digital CD equalization module, which is heavily dispersed in a transmission system without dispersion compensation fibers (DCFs). Therefore, the LO phase noise will significantly influence the performance of the high speed coherent system with only digital CD post-compensation. We note that the EEPN does not exist in a transmission system with entire optical dispersion compensation for instance using DCFs.

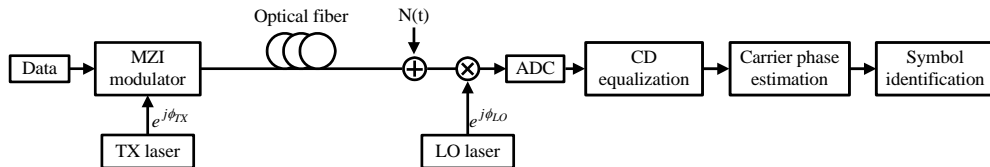


Fig. 1. Scheme of equalization enhanced phase noise in coherent transmission system. MZI: Mach-Zehnder interferometer, Φ_{TX} : phase fluctuation of the TX laser, Φ_{LO} : phase fluctuation of the LO laser, $N(t)$: additive white Gaussian noise, ADC: analog-to-digital convertor.

Theoretical analysis demonstrates that the equalization enhanced phase noise scales linearly with the accumulated chromatic dispersion and the linewidth of the LO laser [14–21], and the variance of the additional noise due to the EEPN can be expressed as follows - see e.g [14]:

$$\sigma_{EEP}^2 = \frac{\pi\lambda^2}{2c} \cdot \frac{D \cdot L \cdot \Delta f_{LO}}{T_s} \quad (1)$$

where λ is the central wavelength of the transmitted optical carrier wave, c is the light speed in vacuum, D is the chromatic dispersion coefficient of the transmission fiber, L is the transmission fiber length, Δf_{LO} is the 3-dB linewidth of the LO laser, and T_s is the symbol period of the transmission system.

It is worth noting that the theoretical evaluation of the enhanced LO phase noise is only appropriate for the FD-FIR and the BLU dispersion equalization, which represent the inverse function of the fiber transmission channel without involving the phase noise mitigation. The analysis of the phase noise enhancement due to the least-mean-square (LMS) adaptive dispersion equalization will be further discussed in a separate publication, and a preliminary example is presented in Section 5.1.

3. Principle of normalized LMS filter for carrier phase estimation

3.1 Principle of normalized LMS filter

The one-tap NLMS filter can be employed effectively for carrier phase estimation [13,27], of which the tap weight is expressed as

$$w_{NLMS}(n+1) = w_{NLMS}(n) + \frac{\mu_{NLMS}}{|x_{PN}(n)|^2} x_{PN}^*(n) e_{NLMS}(n) \quad (2)$$

$$e_{NLMS}(n) = d_{PE}(n) - w_{NLMS}(n) \cdot x_{PN}(n) \quad (3)$$

where $w_{NLMS}(n)$ is the complex tap weight, $x_{PN}(n)$ is the complex magnitude of the input signal, n represents the number of the symbol sequence, $d_{PE}(n)$ is the desired symbol, $e_{NLMS}(n)$ is the estimation error between the output signals and the desired symbols, and μ_{NLMS} is the step size parameter.

It has been demonstrated that the one-tap NLMS carrier phase estimation can be implemented by using the feed-forward control scheme [13]. Therefore, it is not difficult to implement the NLMS-CPE in a parallel-processing circuit for the real-time QPSK coherent transmission system.

3.2 BER floor of phase estimation using NLMS filter with EEPN

The phase estimation using the one-tap NLMS filter resembles the performance of the ideal differential detection [13,28–30], of which the BER floor can be approximately described by an analytical expression (see Appendix):

$$BER_{floor}^{NLMS} \approx \frac{1}{2} \operatorname{erfc} \left(\frac{\pi}{4\sqrt{2}\sigma} \right) \quad (4)$$

$$\sigma^2 \approx \sigma_{TX}^2 + \sigma_{LO}^2 + \sigma_{EEP}^2 \quad (5)$$

$$\sigma_{TX}^2 = 2\pi\Delta f_{TX} \cdot T_s \quad (6)$$

$$\sigma_{LO}^2 = 2\pi\Delta f_{LO} \cdot T_s \quad (7)$$

where σ^2 represents the total phase noise variance in the coherent transmission system, σ_{TX}^2 and σ_{LO}^2 are the original phase noise variance of the transmitter and the LO lasers respectively, and Δf_{TX} is the 3-dB linewidth of the transmitter laser.

It should be noted that the variance of the original TX and LO phase noise are also considered in our derivation in addition to the enhanced LO phase noise included in the total phase noise. The deduction of the EEPN does not consider the intrinsic phase fluctuation from the TX and the LO lasers (see e.g [14].). We assume that the intrinsic TX laser, LO laser phase noise and the EEPN are statistically independent. This assumption is reasonable for practical communication systems with the transmission fiber length over 80 km, which will be discussed in Section 6.2. Therefore, the total phase noise variance can be calculated as the summation of the above three items. The BER floor of phase estimation using the one-tap NLMS filter with EEPN is shown in Fig. 2, which is obtained from Eq. (4). In Fig. 2(a), we could see that the BER floor rises with the increment of the fiber length and the LO laser linewidth, which demonstrates that the EEPN influences the performance of the high speed coherent transmission system significantly. Figure 2(b) indicates the BER floor in phase estimation for different combination of TX and LO lasers linewidth while keeping the sum of linewidths $\Delta f_{TX} + \Delta f_{LO}$ constant. To make the BER floor induced by only the TX phase noise be above 10^{-9} , we need to select a large value (76 MHz and 122 MHz) of the laser linewidth in Fig. 2(b), which may not be used in the practical case. It can be found clearly that the EEPN arises from the LO phase noise, because the BER floor does not change with the increment of fiber length when there is only phase fluctuation from the TX laser. Theoretical investigation demonstrates that the enhanced LO phase noise plays the dominant role in total phase fluctuation, when the accumulated fiber dispersion is larger than 700 ps/nm (about 45 km normal transmission fiber) [14,16].

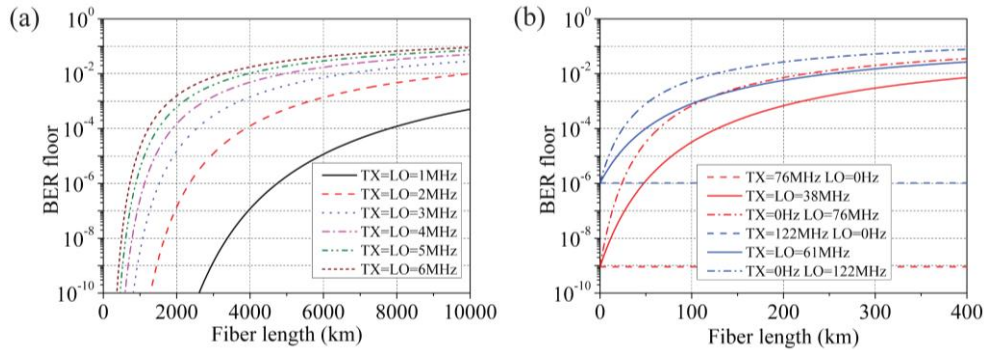


Fig. 2. BER floor of phase estimation in 112-Gbit/s coherent PDM-QPSK transmission system with EEPN. (a) TX laser linewidth is equal to LO laser linewidth, (b) different combination of TX and LO lasers linewidth while keeping the sum of linewidths $\Delta f_{TX} + \Delta f_{LO}$ constant.

3.3 Optimization of the step size in NLMS filter

According to the reported investigation, the step size μ_{NLMS} has an optimal value to provide the best performance of the one-tap NLMS phase estimator for a certain laser phase noise [13]. Roughly speaking, a smaller step size will deteriorate the BER floor induced by the laser phase noise due to the fast phase changing occurring in the long effective symbol average-span. By contrast, a larger step size will degrade the NLMS phase estimator on the sensitivity of optical signal-to-noise ratio (OSNR), but influence the BER floor induced by the phase fluctuation little. The performance of the one-tap NLMS-CPE using different step size is shown in Fig. 3, where both of the TX and LO lasers linewidths are 5 MHz, and the fiber length is 2000 km. We

can see that the one-tap NLMS-CPE shows the best performance when using the optimum step size ($\mu=0.25$), and the BER floor in NLMS-CPE is deteriorated obviously when the smaller step size ($\mu=0.025$) is used. Meanwhile, we find that only the OSNR sensitivity is degraded while the BER floor has no significant variation, when the larger step size ($\mu=1$) is employed in the one-tap NLMS-CPE. Note that the OSNR value is all defined in 0.1 nm and the penalty between the back-to-back result and the theoretical limit (at $\text{BER}=10^{-3}$) is around 1.8 dB.

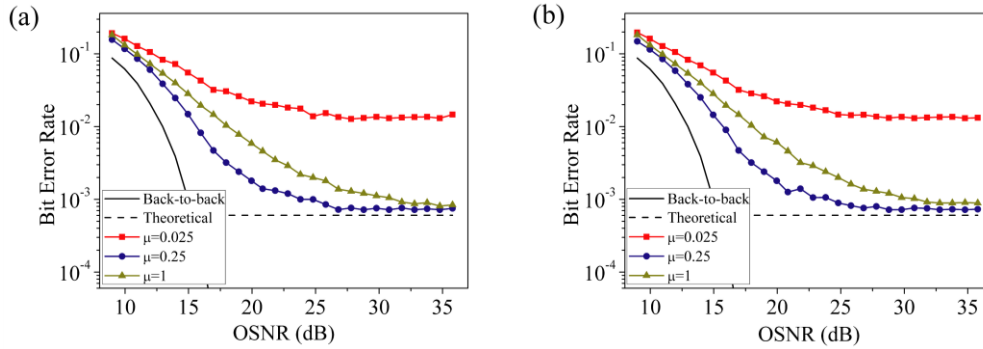


Fig. 3. Phase estimation using the one-tap NLMS filter with different value of step size, μ is the step size. (a) NLMS-CPE with FD-FIR dispersion equalization, (b) NLMS-CPE with BLU dispersion equalization.

From the above analysis, it is important to determine the optimum step size in the application of the one-tap NLMS phase estimation. Corresponding to the definition of the original phase noise from TX and LO lasers, we employ an effective linewidth Δf_{Eff} to describe the total phase noise in the coherent system with EEPN, which can be defined as the following expression:

$$\Delta f_{\text{Eff}} = \frac{\sigma_{\text{TX}}^2 + \sigma_{\text{LO}}^2 + \sigma_{\text{EEP N}}^2}{2\pi T_s}. \quad (8)$$

In Fig. 4(a), we studied the optimum step size for different effective linewidth in the 112-Gbit/s NRZ-PDM-QPSK coherent optical transmission system, which is applicable for both the FD-FIR filter and the BLU filter. It is found that the optimum step size increases with the effective laser linewidth. Note that the one-tap NLMS filter is employed with the optimum step size value for phase estimation in our simulation work.

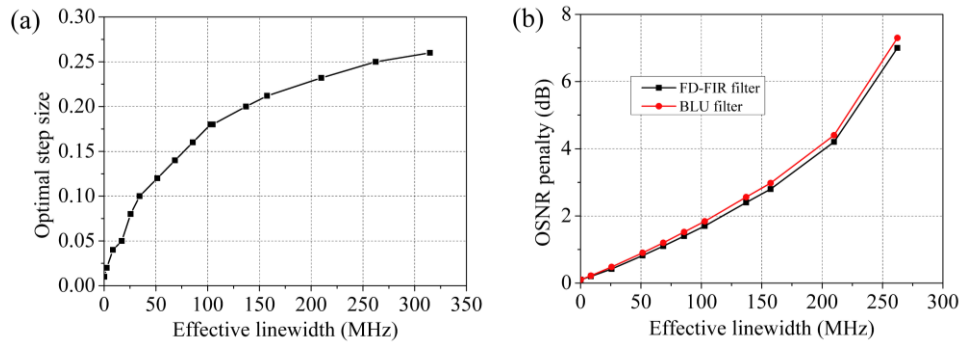


Fig. 4. The optimum step size and the OSNR penalty in NLMS-CPE. (a) optimum step size for different effective linewidth, (b) OSNR penalty in NLMS phase estimation with the optimum step size for FD-FIR and BLU equalization.

Using the FD-FIR and the BLU dispersion equalization, the OSNR penalty from back-to-back result at $\text{BER}=10^{-3}$ in the one-tap NLMS-CPE with the optimum step size are illustrated in Fig. 4(b). It is found that the OSNR penalty scales exponentially with the increment of the effective laser linewidth.

It can be found in Fig. 3 and Fig. 4(b) that the coherent system using the FD-FIR and the BLU dispersion equalization has closely the same performance in the one-tap NLMS carrier phase estimation. Therefore, we will only analyze one of the two digital filters in our later discussion.

4. Simulation investigation of PDM-QPSK transmission system

The setup of the 112-Gbit/s NRZ-PDM-QPSK coherent transmission system implemented in the VPI simulation platform is illustrated in Fig. 5. The data sequence output from the four 28-Gbit/s pseudo random bit sequence (PRBS) generators are modulated into two orthogonally polarized NRZ-QPSK optical signals by the two Mach-Zehnder modulators. Then the orthogonally polarized signals are integrated into one fiber channel by a polarization beam combiner (PBC) to form the 112-Gbit/s NRZ-PDM-QPSK optical signal. Using a local oscillator in the coherent receiver, the received optical signals are mixed with the LO laser to be transformed into four electrical signals by the photodiodes. The four electrical signals are processed by further using the Bessel low-pass filters (LPFs) with a 3-dB bandwidth of 19.6 GHz. Then they are digitalized by the 8-bit analog-to-digital convertors (ADCs) at twice the symbol rate [31]. The sampled signals are processed by the digital equalizer, and the BER is then estimated from the data sequence of 2^{16} bits. The central wavelength of the transmitter laser and the LO laser are both 1553.6 nm. The standard single mode fibers (SSMFs) with the CD coefficient equal to 16 ps/nm/km are employed in all the simulation work.

Here we neglected the influences of fiber attenuation, polarization mode dispersion and nonlinear effects in our simulation. The PMD and polarization rotation equalization could be realized by employing the adaptive LMS and constant modulus algorithm (CMA) equalizers [32]. The chromatic dispersion compensation is implemented by using the digital filters with appropriate parameters, which has been analyzed in our previous work [33].

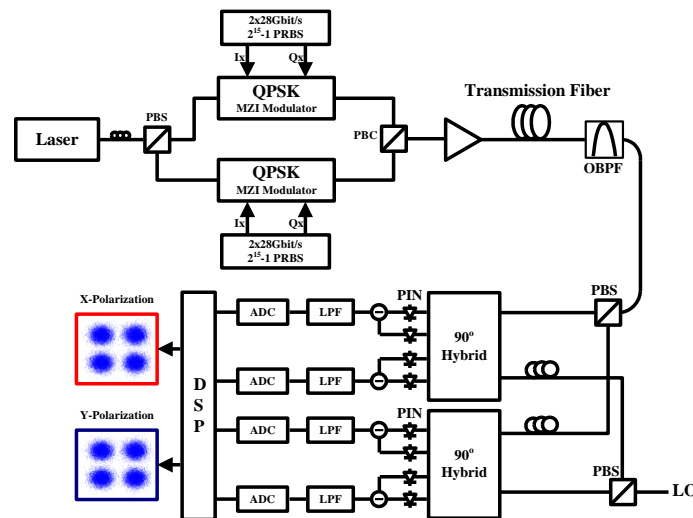


Fig. 5. Schematic of 112-Gbit/s NRZ-PDM-QPSK coherent optical transmission system. PBS: polarization beam splitter, OBPF: optical band-pass filter, PIN: PiN diode.

With the increment of launched optical power, the fiber nonlinearities such as self-phase modulation (SPM), cross-phase modulation (XPM) and four-wave mixing (FWM) need to be considered in the long-haul wavelength-division multiplexing (WDM) transmission systems

[2]. The fiber nonlinear impairments can be mitigated and compensated by using the digital backward propagation methods based on solving the nonlinear Schrodinger (NLS) equation and the Manakov equation [34,35].

5. Simulation results

5.1 Phase estimation considering EEPN with different CD equalization

In Fig. 6, the FD-FIR equalization performance in the coherent transmission system with different fiber length is compared with the adaptive LMS dispersion equalization, where the results are processed by further using a one-tap NLMS filter for carrier phase estimation. The results are obtained under different combination of TX and LO lasers linewidth while keeping the sum of linewidths $\Delta f_{TX} + \Delta f_{LO}$ constant. We can clearly see that influenced by the EEPN, the performance of FD-FIR equalization (the same in BLU equalization) reveals obvious fiber length dependence with the increment of LO laser linewidth. The OSNR penalty in phase estimation scales with the LO phase fluctuation and the accumulated dispersion. On the other hand, the dispersion equalization using the LMS filter shows almost the same behavior in the three cases [27]. That is because the dispersion interplays with the phase noise of both TX and LO lasers simultaneously in the adaptive equalization. Moreover, Fig. 6 also shows that the LMS filter is less tolerant against the phase noise than the other two dispersion equalization methods when carrier phase estimator is employed.

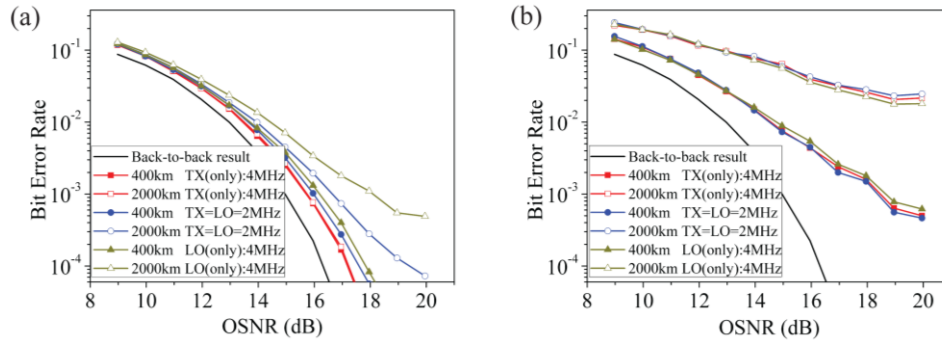


Fig. 6. Carrier phase estimation for various fiber length with different CD compensation methods, where the linewidth of the TX and the LO lasers are in different combination while keeping the sum of linewidths constant. (a) FD-FIR filter, (b) LMS filter.

5.2 Evaluation of BER floor in phase estimation with EEPN

In Fig. 7, the performance of carrier phase estimation using the one-tap NLMS filter with the FD-FIR dispersion equalization is compared with the theoretical evaluation using Eq. (4).

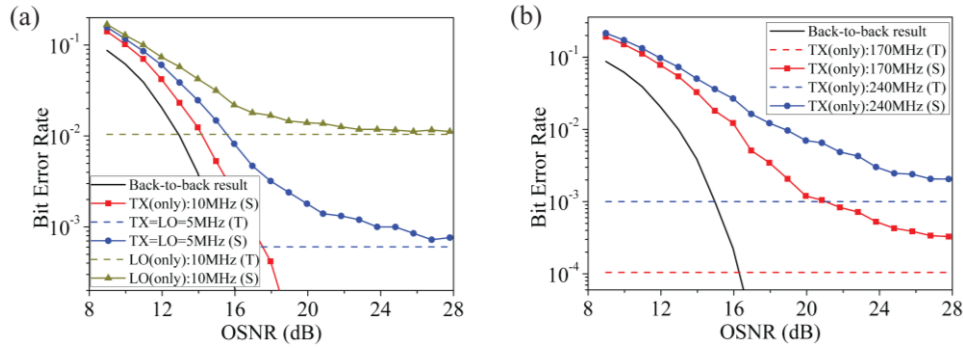


Fig. 7. BER performance in NLMS-CPE for 2000 km fiber with FD-FIR dispersion equalization, T: theory, S: simulation. (a) different combination of TX and LO lasers linewidth while keeping the sum of linewidths constant, (b) only TX laser phase noise.

Figure 7(a) illustrates the numerical results for different combination of TX and LO lasers linewidth while keeping the sum of linewidths $\Delta f_{TX} + \Delta f_{LO}$ constant. With the increment of OSNR value, the numerical simulation reveals the BER floor only influenced by the phase noise, which achieves a good agreement with the theoretical evaluation. Figure 7(b) denotes the results with only the analysis of TX laser phase noise, where a slight deviation is found between the simulation results and the theoretical analysis. It arises from the approximation in the analytical evaluation of the one-tap NLMS phase estimator in Eq. (4), of which only the leading order is considered. It has been validated in our simulation work that the phase estimation with the BLU dispersion equalization performs closely the same behavior as the FD-FIR equalization.

6. Differential phase detection

6.1 Differential QPSK demodulation system

The coherent optical transmission system can be operated in differential demodulation mode when the differential encoded data is recovered by a simple “delay and multiply algorithm” in the electrical domain. In such a case the encoded data is recovered from the received signal based on the phase difference between two consecutive symbols, i.e. the value of the complex decision variable $\Psi = Z_k Z_{k+1}^* \exp\{i\pi/4\}$, where Z_k and Z_{k+1} are the consecutive k-th and (k+1)-th received symbols. The BER floor of the differential phase receiver can be evaluated using the principle of conditional probability [28], which is expressed as the following equation:

$$BER_{floor}^{DQPSK} = \frac{1}{2} \operatorname{erfc}\left(\frac{\pi}{4\sqrt{2}\sigma}\right). \quad (9)$$

The BER performance of the 28-Gsymol/s DQPSK coherent transmission system with the FD-FIR dispersion equalization is illustrated in Fig. 8. Figure 8(a) shows the simulation results for different combination of TX and LO lasers linewidth while keeping the sum of linewidths $\Delta f_{TX} + \Delta f_{LO}$ constant, and Fig. 8(b) denotes the performance of the differential demodulation system with only the TX laser phase noise. It is found that the BER behavior in the DQPSK coherent system can achieve a good agreement with the theoretical evaluation in Eq. (9) for both Fig. 8(a) and Fig. 8(b). The consistence between simulation and theory in DQPSK demodulation is better than the one-tap NLMS phase estimation in the case of only TX laser phase noise.

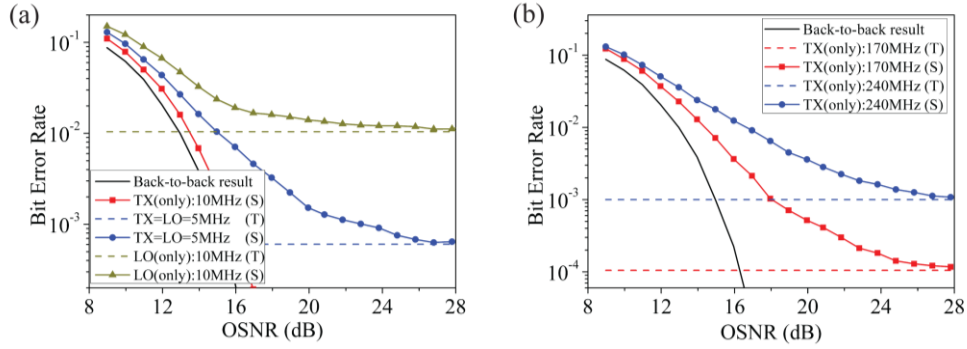


Fig. 8. BER performance in DQPSK system for 2000 km fiber with FD-FIR dispersion equalization, T: theory, S: simulation. (a) different combination of TX and LO lasers linewidth while keeping the sum of linewidths constant. (b) only TX laser phase noise.

6.2 Correlation between EEPN and intrinsic LO phase noise

In the evaluation for the BER floor of the one-tap NLMS phase estimation in Section 3.2, we have assumed that the intrinsic TX laser, LO laser phase noise and the equalization enhanced phase noise are statistically independent. Obviously, the TX laser phase noise is independent from the LO laser phase noise and the EEPN. Here we mainly investigate the correlation between the intrinsic LO laser phase noise and the EEPN. The total phase noise variance in the coherent optical transmission system can be modified as

$$\sigma^2 = \sigma_{TX}^2 + \sigma_{LO}^2 + \sigma_{EEP N}^2 + 2\rho \cdot \sigma_{LO} \sigma_{EEP N} \quad (10)$$

where ρ is the correlation coefficient between the intrinsic LO laser phase noise and the EEPN, and we have the absolute value $|\rho| \leq 1$.

We have implemented the numerical simulation in the DQPSK system for different combination of the intrinsic LO laser phase noise and the EEPN while keeping a constant sum, which is illustrated in Fig. 9(a). It can be found that the BER floor does not show tremendous variation due to the correlation between the LO laser phase noise and the EEPN. The BER floor reaches the lowest value at $\sigma_{EEP N}^2 = 0.5\sigma_{LO}^2$, which corresponds to the maximum value of the term $|2\rho \cdot \sigma_{LO} \sigma_{EEP N}|$. The cases for $\sigma_{EEP N}^2 \gg \sigma_{LO}^2$ and $\sigma_{EEP N}^2 = 0$ correspond to the mutual term $|2\rho \cdot \sigma_{LO} \sigma_{EEP N}| = 0$. From Fig. 9(a) we can find that ρ is usually a negative value.

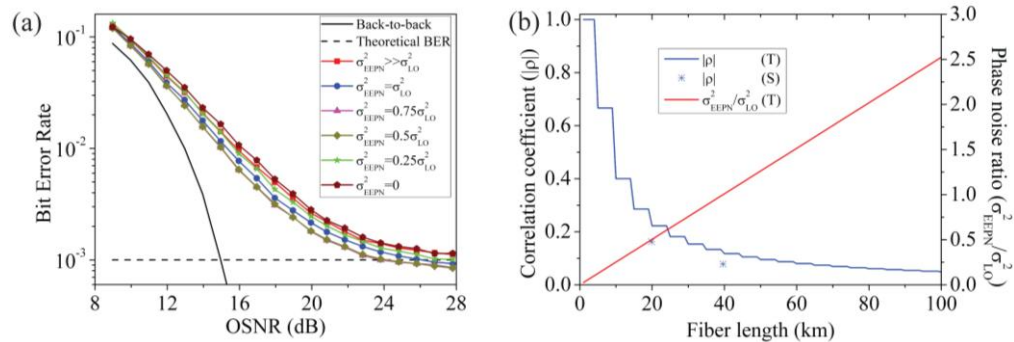


Fig. 9. Phase noise correlation in DQPSK system with BLU dispersion equalization, T: theory, S: simulation. (a) BER performance in different combination of EEPN and LO phase noise but keeping the same sum, (b) correlation coefficient for different fiber length.

The EEPN arises from the electronic dispersion compensation where the phase of the equalized symbol fluctuates during the time window of the digital filter, while the intrinsic LO laser phase fluctuation comes from the integration during the consecutive symbol period. Therefore, we could give an approximate theoretical evaluation of the correlation coefficient as

$$|\rho| \approx \frac{T_s}{N \cdot T}. \quad (11)$$

where N is the required tap number (or the necessary overlap) in the chromatic dispersion compensation filter, and T is the sampling period in the transmission system. The tap number (or the necessary overlap) can be calculated by the fiber dispersion to be compensated [22,25], and the sampling period $T = \frac{1}{2}T_s$ when the sampling rate in the ADC modules is selected as twice the symbol rate.

The absolute value of the correlation coefficient $|\rho|$ for different fiber length is illustrated in Fig. 9(b), in which we can see that the correlation coefficient $|\rho|$ determined from the numerical simulation achieves good agreement with the theoretical approximation. With the increment of fiber length, the magnitude of correlation coefficient $|\rho|$ approaches zero rapidly. Consequently, we can neglect the correlation term in Eq. (10) when the fiber length is over 80 km. Therefore, the assumption in Eq. (5) is valid when the fiber length exceeds 80 km in practical optical communication systems. A more accurate analytical expression for correlation coefficient could be derived from the mathematical definition of correlation between two random variables by using the probability density functions (PDFs) of the LO phase noise and the EEPN [9,16]. This will be studied in our future work.

Note that in Fig. 9 we use the BLU dispersion equalization rather than the FD-FIR equalization, because we need to employ various fiber length for different combination of the LO laser phase noise and the EEPN, while the FD-FIR filter shows the malfunctioned performance for short distance fibers [33].

7. Conclusions

To evaluate the impact of the dispersion equalization enhanced phase noise, two electronic dispersion equalizers involving the FD-FIR filter and the BLU filter are applied to compensate the CD in the 112-Gbit/s NRZ-PDM-QPSK coherent optical transmission system. The carrier phase estimation is implemented by using the one-tap normalized LMS filter, of which the performance is analyzed in detail. The BER floor of the one-tap NLMS phase estimation with the enhanced phase noise is analytically evaluated, and the simulation results are compared to the differential phase detection system. As a novel result, it is found that the FD-FIR and the BLU dispersion equalization with the one-tap NLMS carrier phase estimation have very similar phase noise statistic performance as using differential phase detection. The small deviation of significance for shorter transmission distance (when the EEPN is small) is tentatively attributed to the high order analysis in the NLMS phase estimation. We have for the first time evaluated the correlation between the LO phase noise and the EEPN in detail, and have given a novel quantitative explanation for the size of the correlation. It is verified that the correlation effect is only of practical significance for the transmission distance less than 80 km normal transmission fiber.

The evaluation of the BER floor in phase estimation with the LMS adaptive dispersion equalization is rather complicated due to the equal enhancement of both TX and LO lasers phase noise as shown in the simulation example. This will be investigated in our future work. Moreover, the effects of EEPN on different phase estimation algorithms in coherent transmission system will be also studied in the future investigations.

Appendix: BER floor of phase estimation using one-tap NLMS filter

Assuming that the one-tap NLMS filter has converged through numbers of iterations [27], the k -th output symbol after the carrier phase estimation can be expressed as

$$\begin{aligned} y_{PE}(k) &= w_{NLMS}(k) \cdot x_{PN}(k) \\ &= b_k E_k \exp[j(\phi_k - \Phi_k)] \end{aligned} \quad (A1)$$

$$x_{PN}(k) = E_k \exp(j\phi_k) \quad (A2)$$

$$w_{NLMS}(k) = b_k \exp(-j\Phi_k) \quad (A3)$$

$$e_{NLMS}(k) = d_{PE}(k) - y_{PE}(k) \quad (A4)$$

where $x_{PN}(k)$ is the k -th received symbol, $y_{PE}(k)$ is the k -th output symbol after the carrier phase estimation, $w_{NLMS}(k)$ is the k -th tap weight in the one-tap NLMS filter, E_k is the complex envelope of the electrical field of the received symbol, ϕ_k is the total phase fluctuation in the received symbol, b_k is a positive real coefficient of tap weight, Φ_k is the estimated phase in the one-tap NLMS filter.

To achieve a satisfactory effect of phase noise compensation, we have the estimated error:

$$|e_{NLMS}(k)| \ll 1. \quad (A5)$$

Namely, we have the estimated phase as

$$\Phi_k \approx \phi_k. \quad (A6)$$

Therefore, for the $(k+1)$ -th received symbol, the $(k+1)$ -th output symbol after the CPE can be describes as following equations:

$$\begin{aligned} y_{PE}(k+1) &= w_{NLMS}(k+1) x_{PN}(k+1) \\ &\approx \left[b_k E_{k+1} + \frac{\mu_{NLMS}}{|E_k|^2} e_{PE}(k) E_k^* E_{k+1} \right] \cdot \exp[j(\phi_{k+1} - \phi_k)], \end{aligned} \quad (A7)$$

$$x_{PN}(k+1) = E_{k+1} \exp(j\phi_{k+1}), \quad (A8)$$

$$w_{NLMS}(k+1) = w_{NLMS}(k) + \frac{\mu_{NLMS}}{|x_{PN}(k)|^2} e_{PE}(k) x_{PN}^*(k). \quad (A9)$$

It is found that the function of the one-tap NLMS filter resembles the ideal differential detection. The BER floor in the one-tap NLMS-CPE can be calculated correspondingly [28–30], which is described as the following expression:

$$BER_{floor}^{NLMS} \approx \frac{1}{2} \operatorname{erfc} \left(\frac{\pi}{4\sqrt{2}\sigma} \right). \quad (A10)$$

The BER floor in phase estimation using the one-tap NLMS filter with different phase noise variance is illustrated in Fig. 10.

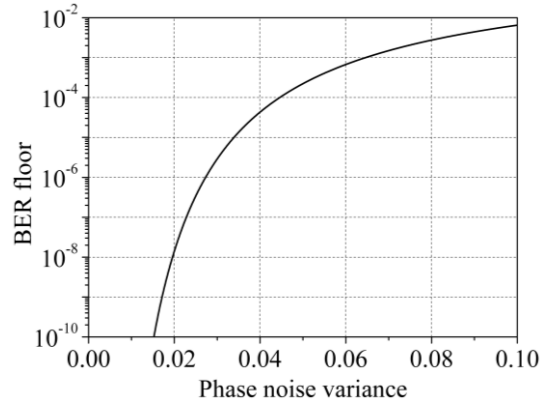


Fig. 10. BER floor of phase estimation using one-tap NLMS filter.